The EMBO Journal Vol.16 No.7 pp.1484–1491, 1997

The tertiary structural changes in bacteriorhodopsin occur between M states: X-ray diffraction and Fourier transform infrared spectroscopy

H.J.Sass[1], I.W.Schachowa, G.Rapp[2], M.H.J.Koch[2], D.Oesterhelt[3], N.A.Dencher[4] and G.Büldt

Forschungszentrum Jülich, IBI-2: Structural Biology, D-52425 Jülich, [2]European Molecular Biology Laboratory, EMBL c/o DESY, Notkestrasse 85, D-22603 Hamburg, [3]Max-Planck-Institut für Biochemie, D-82152 Martinsried and [4]Institut für Biochemie, Abt. Physikalische Biochemie, Technische Hochschule Darmstadt, Petersenstrasse 22, D-64287 Darmstadt, Germany

[1]Corresponding author
e-mail: Jurgen@ibistr.dnet.kfa-juelich.de

The tertiary structural changes occurring during the photocycle of bacteriorhodopsin (BR) are assigned by X-ray diffraction to distinct M states, M_1 and M_2. Purple membranes (PM) of the mutant Asp96Asn at 15, 57, 75 and 100% relative humidity (r.h.) were studied in a parallel X-ray diffraction and Fourier transform infrared (FTIR) spectroscopic investigation. Light-dependent conformational changes of BR-Asp96-Asn are observed at high hydration levels (100 and 75% r.h.) but not in partially dehydrated samples (57 and 15% r.h.). The FTIR spectra of continuously illuminated samples at low and high hydration, despite some differences, are characteristic of the M intermediate. The changes in diffraction patterns of samples in the M_2 state are of the same magnitude as those of wild-type samples trapped with GuaHCl in the M_G state. Additional large changes in the amide bands of the FTIR spectra occur between M_2 and M_G. This suggests, that the tertiary structural changes between M_1 and M_2 are responsible for the switch opening the cytoplasmic half-channel of BR for reprotonation to complete the catalytic cycle. These tertiary structural changes seem to be triggered by a charge redistribution which might be a common feature of retinal proteins also in signal transduction.

Keywords: conformational changes/hydration/ M intermediates/photocycle/proton pumping

Introduction

Changes in the tertiary structure of the membrane protein bacteriorhodopsin (BR) during the transition from its ground state to the photocycle intermediate M have been observed by neutron (Dencher *et al.*, 1989), X-ray (Dencher *et al.*, 1991; Koch *et al.*, 1991; Nakasako *et al.*, 1991) and electron diffraction (Subramaniam *et al.*, 1993; Han *et al.*, 1994). A concomitant increase of the lattice constant of the purple membranes (PM) in the range between 0.2 and 0.5% also occurs with the transition to the M intermediate (Dencher *et al.*, 1989; Koch *et al.*, 1991. Nakasako *et al.*, 1991).

The spectroscopic transition of BR to its M intermediate is characterized by a shift of the absorption maximum of the retinal chromophore from 570 nm in the light-adapted ground state to 410 nm. This shift results from the all-*trans* to 13-*cis* isomerization of the retinal, the deprotonation of its Schiff base linkage and the concomitant protonation of amino acid Asp85. Thereafter a proton is released at the extracellular side of the membrane (Dencher *et al.*, 1991). The next intermediates of the photocycle, called N and O, are relaxation processes leading to the restoration of the ground state. With the transition to the N intermediate, the Schiff base is reprotonated from the Asp96, which is located on the cytoplasmic side of the proton wire, whereas re-isomerization of the retinal and reprotonation of Asp96 occur with the transition to the O state. The initial state which is finally reached is characterized by a protonated Schiff base, a protonated Asp96 and a deprotonated Asp85 (for reviews, see Oesterhelt *et al.*, 1992; Ebrey, 1993; Lanyi, 1995).

The M intermediate formed under release of a proton towards the extracellular side decays with the reprotonation from the intracellular side via Asp96. Thus, two M states must exist with different p*K* values and accessibilities of the Schiff base for the proton, conveniently called M_1 and M_2. The switch in accessibility must be due to conformational changes of the protein and/or the retinylidene moiety (Schulten and Tavan, 1978; Fodor *et al.*, 1988). To describe the kinetics of the photocycle, Varo and Lanyi (1990, 1991a) postulated an irreversible transition between M_1 and M_2. This could not, however, hitherto be unambiguously proven experimentally, although the presence of two M intermediates (M_1 and M_2) had been deduced much earlier from spectroscopic measurements (Korenstein *et al.*, 1978).

UV-VIS (Varo and Lanyi, 1991b; Varo *et al.*, 1992; Zimanyi *et al.*, 1992) and Fourier transform infrared (FTIR) spectroscopy (Ormos, 1991; Perkins *et al.*, 1992) revealed a transition from M_1 to M_2 by a slight shift in the absorption maximum of the M intermediate and changes in the amide-I region (1650–1670 cm^{-1}), respectively. Later, the FTIR results were, however, re-interpreted as giving no evidence for a M_1 to M_2 transition, due to doubts about the purity of the accumulated substates (Ormos *et al.*, 1992; Vonck *et al.*, 1994).

Different procedures have been used to generate the M intermediate: (i) cooling wild-type BR to a temperature between 220 and 260 K before illumination (Ormos, 1991); (ii) incubation of wild-type BR with guanidine hydrochloride (GuaHCl) at pH 9.6 (Dencher *et al.*, 1989); and (iii) using the BR mutant Asp96Asn (BR-D96N), which displays a pH-dependent retardation of the M decay (Butt *et al.*, 1989; Koch *et al.*, 1991; Subramaniam *et al.*, 1993). Dehydration of the PM is also known to influence the kinetics of the photocycle and especially retards the

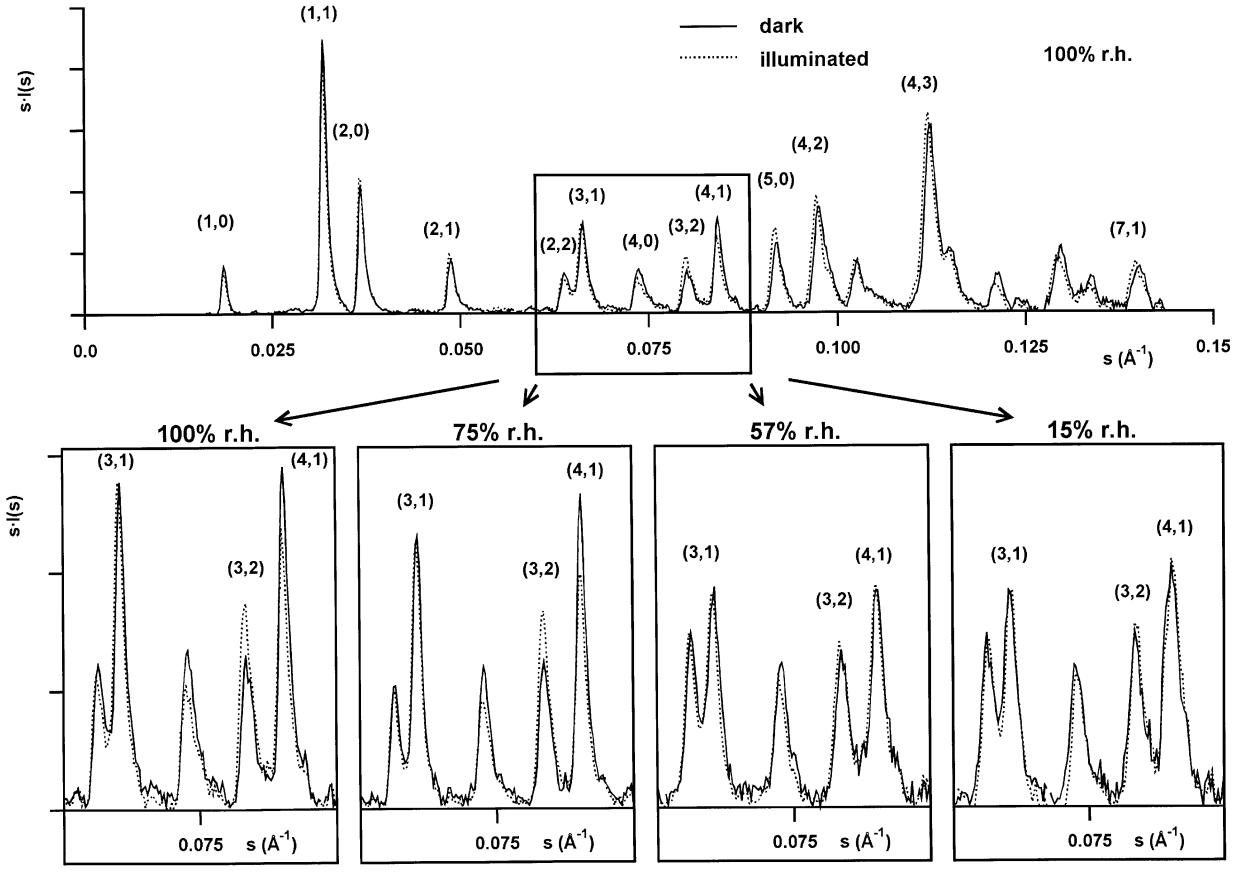

Fig. 1. Lorentz-corrected X-ray diffraction patterns of BR-D96N light-adapted purple membranes (pH 9.6, room temperature) at different hydration levels in the absence of light (solid line) and under steady-state illumination (dotted line). $s = 2\sin\Theta/\lambda$, with Bragg angle Θ and wavelength $\lambda = 1.5$ Å. The lower panels represent the reflection range (2,2) to (4,1) at different r.h. on an expanded scale.

decay of the M intermediate (Korenstein and Hess, 1977; Varo and Lanyi, 1991c; Thiedemann *et al.*, 1992).

To clarify whether the changes in the tertiary structure of the protein take place at the onset of the M intermediate or with the transition between M states, we have performed a combined FTIR and X-ray diffraction study on BR-D96N samples trapped in the M intermediate at different degrees of hydration. Comparison of these trapped M states with that of wild-type M obtained by cooling or by incubation with GuaHCl led to the conclusion that the changes in the tertiary structure of BR occur during the M_1 to M_2 transition. Furthermore, it could be demonstrated that the large structural changes reflected in the diffraction experiments are not identical to the largest changes in the amide bands of the FTIR difference spectra. The light-induced alteration of the tertiary structure, especially the changes in the vicinity of helix F and G, are only detectable under conditions which allow the release of the proton to the extracellular side of the membrane. This indicates that proton translocation initiates the structural changes by a charge redistribution.

Results

Tertiary structural changes seen by X-ray diffraction

The X-ray diffraction patterns of the BR-D96N mutant at different hydration levels in the ground-state and during steady-state illumination are shown in Figure 1. The characteristic changes accompanying the transition from the ground-state to the M intermediate are most pronounced in the (3,2) and (4,1) reflections of the samples with hydration at or above 75% relative humidity (r.h.). At lower r.h. the intensity differences become small. This is illustrated further by the difference electron density maps in Figure 2, demonstrating the presence (75% r.h.) and the absence (57% r.h.), respectively, of a pronounced density increase at helix F, G and B in the M intermediate as reported in previous publications (Dencher *et al.*, 1989, 1991; Koch *et al.*, 1991; Nakasako *et al.*, 1991; Subramaniam *et al.*, 1993; Han *et al.*, 1994). Both the hydrated and the dry samples are in the M state during continuous illumination, as indicated by their colour change from purple to yellow. The intensity of the (3,1) reflection decreases continuously between 100 and 57% r.h. and then remains nearly constant. It does not change upon illumination independently of hydration. This makes it a good marker of the hydration level and allows us to exclude that the changes between the dark and illuminated samples would be due to an artificial transient dehydration.

M states of the hydrated and dehydrated samples

The FTIR difference spectra of BR-D96N and wild-type samples with hydration levels comparable with those of the X-ray experiments are shown in Figures 3 and 4. The spectra clearly illustrate that the M states of the hydrated (100 and 75% r.h.) and dry (50 and 38% r.h.) samples differ mainly in the amide bands, at 1650–1670 cm^{-1} (amide-I region)

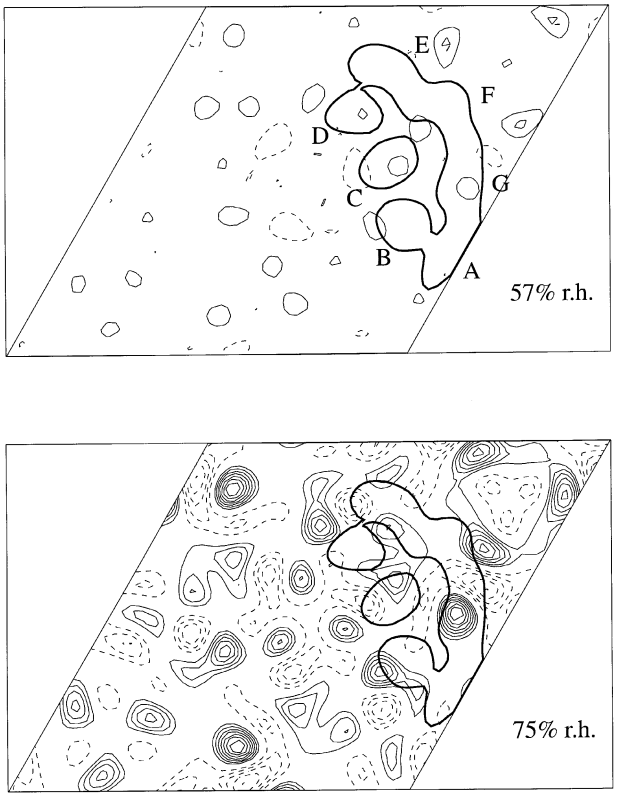

Fig. 2. Difference electron density maps (M state minus light-adapted ground state) of the BR-D96N purple membranes at different hydration levels. Top: 57% r.h., M_1 state. Bottom: 75% r.h., M_2 state. The bold contour outlines the BR monomer, individual helices are marked by upper case letters from A to G. Continuous lines correspond to positive, dashed lines to negative electron density levels. Contour levels are scaled to each other in both maps.

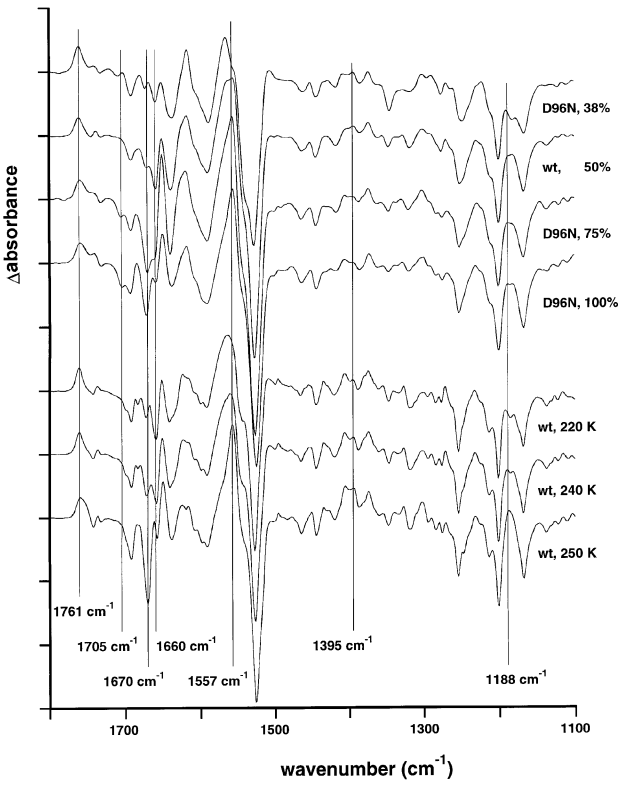

Fig. 3. FTIR difference spectra (M state minus light-adapted ground state). Upper four spectra: BR-D96N (pH 9.6, room temperature) at different levels of hydration and wild-type BR at 50% r.h. Lower three spectra: wild-type BR (pH 10, 100% r.h.) at different temperatures. Successive spectra, all having zero value at 1800 cm^{-1}, were displaced by 0.01 units along the ordinate for better visualization.

and 1540–1560 cm^{-1} (amide-II region). The most obvious difference lies in the ratio of the intensities at 1670 and 1660 cm^{-1}, which is <1 in the dry samples and >1 in the hydrated samples. The increase in relative humidity is also accompanied by a qualitative change in the appearance of the amide-II band.

Additional differences are also detectable in the amide-I region of the various dry samples. The intensity of the amide-I band is clearly lower at the lowest hydration (38% r.h.) than in the sample at 50% r.h., although the other bands, especially those at 1761, 1640 and 1620 cm^{-1}, are similar. All difference spectra of these samples display a positive band around 1761 cm^{-1}, indicative of the protonation of Asp85. The negative band around 1640 cm^{-1} and the positive band around 1620 cm^{-1} are characteristic of the deprotonation of the Schiff base. Also the fingerprint region (C–C stretch of the retinal) of the difference spectra of all these samples exhibits negative values at 1188 cm^{-1}, giving further evidence for the M intermediate (Braiman *et al.*, 1987; Gerwert *et al.*, 1989; Pfefferle *et al.*, 1991). Even at the lowest hydration level investigated here, the difference bands characteristic of the M intermediate are clearly observed. The dry samples used for the X-ray experiments are thus also trapped in the M intermediate.

M states at different temperatures

Beside the mutant samples at different hydrations, difference spectra of BR wild-type samples at 220, 240 and 250 K are also presented in Figures 3 and 4. The direct comparison illustrates similarities in the changes found for M states trapped either by cooling or dehydration. As already observed by Ormos (1991), samples trapped in the M state at temperatures of 240 K and below have an amide-I ratio (1670:1660 cm^{-1}) <1, whereas above 240 K this ratio is >1. In contrast to the spectra of the mutant at 100% r.h. and of wild-type at or below 240 K, the spectrum of wild-type BR at 250 K gives clear indications of contributions from the N intermediate. These are mainly the asymmetric broadening of the difference band at 1761 cm^{-1} towards 1755 cm^{-1}, the appearance of a negative band at 1742 cm^{-1} and of a positive band region around 1390–1400 cm^{-1}, as well as an increase in the band at 1188 cm^{-1} (Pfefferle *et al.*, 1991). These observations are in agreement with those which led Ormos *et al.* (1992) to reject the existence of different M states as an explanation for the changes observed at different temperatures. The changes in the amide-I and amide-II regions of wild-type BR at 250 K cannot, however, simply be due to a contamination of the trapped M state by the N intermediate, since the same pattern is seen in the hydrated BR-D96N samples, where no indications of N state contributions are detectable in the FTIR difference spectrum (Figure 3).

Similar X-ray diffraction and FTIR observations were made on BR-D96N embedded in glucose at different levels of hydration (data not shown). They demonstrate that glucose has less influence on the M intermediate than

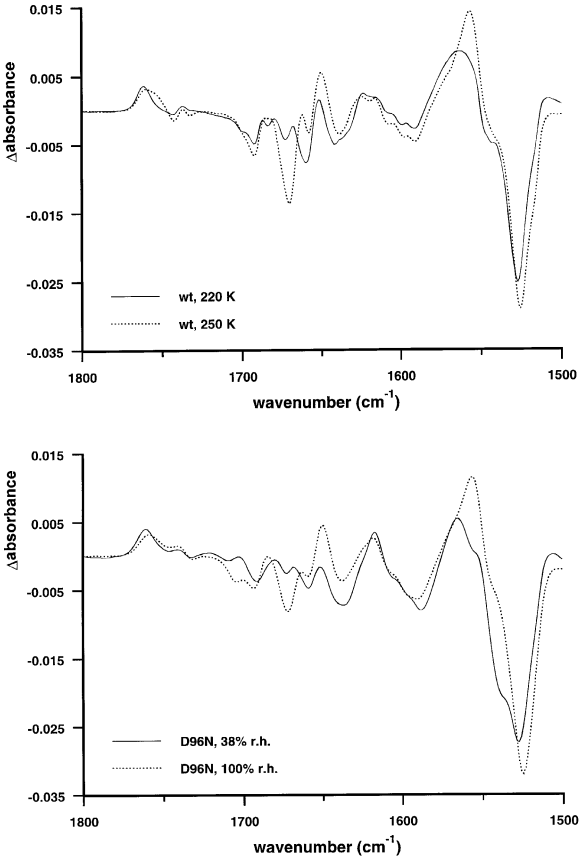

Fig. 4. Top: expanded carboxy, amide-I and amide-II region of the wild-type samples (pH 10, 100% r.h.) at 220 and 250 K. Bottom: carboxy, amide-I and amide-II region of the BR-D96N samples (pH 9.6, room temperature) at different levels of hydration (38 and 100% r.h.).

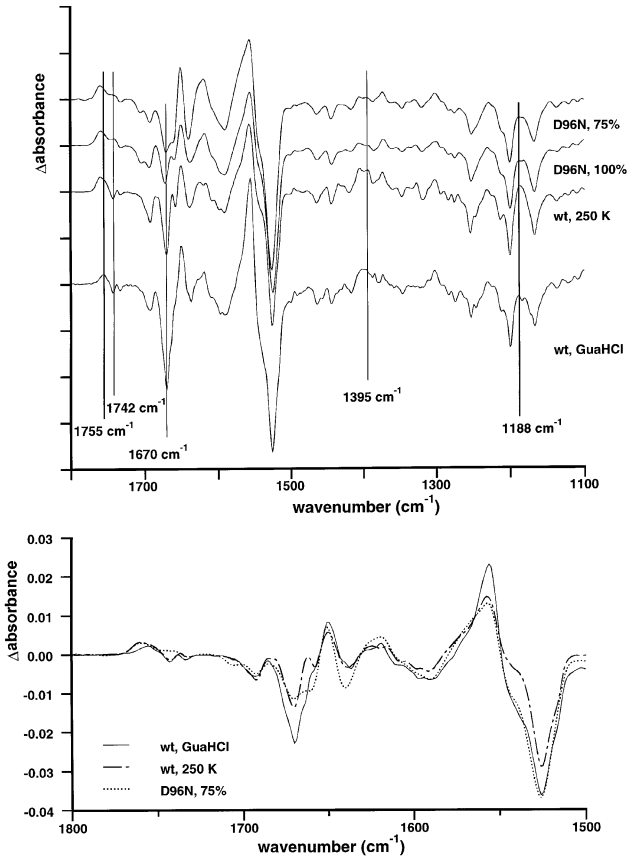

Fig. 5. FTIR difference spectra (M state minus light-adapted ground state). Top: BR-D96N at 75 and 100% r.h., wild-type BR incubated with GuaHCl and BR at 250 K. The successive spectra, all having zero value at 1800 cm^{-1}, were displaced by 0.01 units along the ordinate for better visualization. Bottom: expanded carboxy, amide-I and amide-II regions.

the actual hydration of the sample, as already suggested by Vonck *et al.* (1994).

The M state trapped with GuaHCl

A comparison of all FTIR difference spectra with an amide-I ratio (1670:1660 cm^{-1}) >1 with those of a BR wild-type sample incubated with GuaHCl is presented in Figure 5. The latter spectrum clearly displays all characteristic difference bands assigned earlier by Sasaki *et al.* (1992) to a state which was called M_N to indicate the presence of the amide-I and -II band patterns characteristic of the N state without any indication of the reprotonation of the Schiff base. It should be noted that the difference spectra of the M_N state presented here were obtained without additional subtraction of a 'pure M' difference spectrum from the measured difference spectrum, as described in earlier work (Sasaki *et al.*, 1992).

The wild-type sample incubated with GuaHCl also showed a negative band at 1742 cm^{-1}, indicating the deprotonation of Asp96. Therefore, we call this M_N-like state M_G. The FTIR difference spectrum of this final substate of the M intermediate is characterized by a shifted positive band for Asp85 (1755 cm^{-1}), a negative band at 1742 cm^{-1} and large changes in the amide-I (1650, 1670 cm^{-1}) and the amide-II region (~1555 cm^{-1}) compared with the other M spectra. In contrast, none of the characteristic changes in the fingerprint region at 1188 cm^{-1} nor in the region of the protonated Schiff base NH bending (1395 cm^{-1}), indicative of the reprotonation of the Schiff base and hence of the N intermediate, are detectable.

Discussion

The structures of the M_1 and M_2 states

Both the X-ray diffraction and FTIR results point to the existence of distinct states in the M intermediate of the BR photocycle. The hydrated samples (100 and 75% r.h., Figure 1) display the same changes in the intensities of the diffraction pattern as reported previously (Dencher *et al.*, 1989, 1991; Koch *et al.*, 1991; Nakasako *et al.*, 1991; Subramaniam *et al.*, 1993), whereas almost no intensity changes are detectable in the diffraction patterns of the less hydrated samples (57 and 15% r.h.) upon illumination. These dry samples are, however, also trapped in the spectroscopic M intermediate, as judged from their colour and FTIR spectra obtained under identical conditions. The changes in the tertiary structure during the transition from one M state to another determined above are in line with the recently reported differences in the activation volume between the L to M_1 and M_1 to M_2 transitions (Varo and Lanyi, 1995), indicating that major changes occur between M_1 and M_2.

In parallel, there are also clear differences in the amide-I

region of the FTIR difference spectra of the dry and hydrated samples, in particular in the peak amplitude ratio 1670:1660 cm^{-1}. The latter was originally taken by Ormos (1991) and Perkins *et al.* (1992) as an indication of different M states, M_1 and M_2. Although the interpretation of the FTIR spectra initially supported the hypothesis of the existence of the M_1 and M_2 states (Ormos, 1991; Perkins *et al.*, 1992), it was later revoked by Ormos *et al.* (1992), arguing that the differences in the spectra simply result from a mixture of L and M or M and N intermediates, and modified by Vonck *et al.* (1994), defining the first state as pure M or M_2 and the second as a mixture of M_2 and M_N.

Concerning our X-ray data, we suggest that the initial assignment (Ormos, 1991; Perkins *et al.*, 1992) of the FTIR difference peaks in the amide-I region to the M states M_1 and M_2 was correct, although their samples might have had admixtures of the L or N state respectively. Consequently, we assign our dry samples, exhibiting no changes in the tertiary structure according to our X-ray data, to be in the M_1 state. Since M_1 is supposed to be in equilibrium with the L intermediate, one would expect admixtures of characteristic L difference bands in our FTIR spectra of the dry samples. Obviously this is not the case, as shown in Figure 3 for the mutant sample at 38% r.h. The fingerprint region gives no indication of this; for example, compare the band at 1188 cm^{-1} of this spectrum with the L spectrum published by Heßling *et al.* (1993). However, the absence of admixtures of the L intermediate in the spectra of our dry samples at pH 9.6 does not exclude the assignment of this intermediate as M_1. This is understandable from earlier observations noted in the literature. Varo and Lanyi (1991c) found a decrease in the production of L from M_1 and in the rate constant for the conversion of M_1 to M_2 with decreasing water content. Zimanyi *et al.* (1992) reported a 50-fold acceleration in the L to M_1 reaction at pH 10 compared with pH $\leqslant$8. These results strongly suggest that an accumulation of the M_1 state under the condition of low hydration and high pH occurred in our samples.

Comparison of the low temperature measurements with those at different hydration levels confirms that the changes occurring in the amide regions and hence also the development of the M states in the wild-type BR and in the BR-D96N are comparable, as illustrated in Figure 3. For samples which display an amide-I ratio (1670:1660 cm^{-1}) <1, only small changes in the tertiary structure of the protein are detected in diffraction experiments, whereas large changes occur in all samples displaying an amide-I ratio >1 (Figures 1 and 2). We thus conclude that the change in the peak amplitude ratio is indicative of the transition from one M state to another. The structural changes detected by the diffraction experiments are, however, not correlated with the largest changes in the amide regions which are only fully developed in the M_N state. That is, comparing the amide regions of the sample at 75% r.h. (already showing the full changes in the X-ray structure) with the spectra of wild-type BR incubated with GuaHCl, the latter sample displays not only much larger difference bands in this region, but also different relative values of the difference maxima (1670, 1660 and 1650 cm^{-1}). This reduces the possibility that only the influence of the water content is a pure source of this distinction. In addition, the band of Asp85 at ~1760 cm^{-1} also changes clearly from having a shoulder near 1755 cm^{-1} to having a clear maximum at 1755 cm^{-1} in wild-type BR incubated with GuaHCl. Alltogether, these differences indicate that even assuming an admixture of the M_N state in the spectra of the wet samples, this contribution is not dominating and therefore cannot be the origin of the large structural changes detected with X-ray diffraction. This is true especially if one also considers that there are no further great changes in the diffraction intensity distribution upon illumination between the sample at 75 and 100% r.h. and those of the wild-type BR incubated with GuaHCl. Therefore, we conclude that the structural changes detected with X-ray diffraction are completed before the sample is in the M_N state, i.e. they are already present in the M_2 state.

Conversely, small changes occur in the amide regions before the changes in the diffraction pattern become detectable. The FTIR measurements at different temperatures and different degrees of hydration indicate that the changes in the amide regions develop continuously and can be trapped at different magnitudes. When the difference peak ratio in the amide-I region rises beyond a value of unity, a state is reached where the large structural changes are observed in the diffraction pattern. The IR spectra always unequivocally indicate the protonation of Asp85 (difference band at 1761 cm^{-1}) and the deprotonation of the Schiff base.

These continuous IR changes preceding a large conformational transition can be interpreted by assuming a hierarchy of conformational substates of the M intermediate (Frauenfelder, 1995). These are separated by comparatively low energy barriers and therefore trapped at slightly different temperatures or hydration levels.

At the onset of the M_1 region, no changes in the amide regions are detectable but all features characteristic of a deprotonated Schiff base and a protonated Asp85. Subsequently, some changes develop in the structure of the protein which are accompanied by changes in the amide-I region of the FTIR difference spectra. These smaller structural changes ultimately lead to the conformational transition detected in the diffraction experiments.

For the hydrated samples (75 and 100% r.h.), the characteristic changes associated with the large alteration of the tertiary structure are illustrated in the difference electron density map in Figure 2. They are the same as reported earlier (Dencher *et al.*, 1989, 1991; Koch *et al.*, 1991; Nakasako *et al.*, 1991; Subramaniam *et al.*, 1993) with the main positive peaks near helices B, F and G. The closely apposed negative peaks near helix F were proposed to indicate a net outward movement of this helix away from the central position of the protein. It was shown further that the structural changes are located in the cytoplasmic half of the protein (Subramaniam *et al.*, 1993; Vonck, 1996).

The particular structure of the M_N/M_G state

The differences in the amide regions of the FTIR spectra of the samples at 75 and 100% r.h. suggest that beside the large changes in tertiary structure seen in diffraction, there are additional smaller ones, resulting in large alterations of the FTIR signal, which fully develop until the next intermediate, the N state, is reached. This is in agreement with the proposal of Vonck *et al.* (1994) and Han *et al.* (1994) that the second M state detectable by FTIR spectroscopy is a mixture of M_2 and M_N. The first

evidence for such a mixture of M states came from FTIR investigations on the BR mutant D96N (Sasaki *et al.*, 1992), which demonstrated that at high pH the M difference spectrum is a combination of a pure M spectrum and a spectrum which clearly displays the characteristic difference band pattern of the N state in the amide regions, although the fingerprint region still confirms the existence of the M intermediate. The changes in the amide regions are larger in the M_N state than in the M_1 or M_2 states and similar to those of the N intermediate (Pfefferle *et al.*, 1991; Heßling *et al.*, 1993), as illustrated by the spectrum of the wild-type sample incubated with GuaHCl (Figure 5).

In our previous diffraction experiments on wild-type samples incubated with GuaHCl (Dencher *et al.*, 1991), we found nearly the same changes in the intensities upon illumination as with the hydrated samples of the mutant D96N. The additional changes in the amide regions occurring during the M_2 to M_N transition are thus clearly not correlated with the changes in the tertiary structure detected in the diffraction experiments. This conclusion is supported further by the recent X-ray diffraction experiment by Kamikubo *et al. (*1996) and an electron diffraction investigation by Vonck (1996), demonstrating the same structural changes for the N intermediate as determined before for the M intermediate (Dencher *et al.*, 1989, 1991; Koch *et al.*, 1991; Nakasako *et al.*, 1991). These results (Kamikubo *et al.*, 1996; Vonck, 1996) support the previous conclusion that the tertiary structural changes relax in the catalytic cycle later than in the N intermediate (Dencher *et al.*, 1991; Koch *et al.*, 1991). On the other hand, the clearly different FTIR spectra of the wet BR-D96N and the wild-type sample incubated with GuaHCl indicate that contrary to the assumption of Han *et al.* (1994) and Vonck (1996), the structural changes shown for the BR-D96N sample are those characteristic for M_2 and not for the M_N state.

To understand the above-mentioned differences in the extent of structural changes between the FTIR and X-ray results, it should be noted that structural changes resolved by FTIR are not necessarily large enough to be detectable by diffraction methods at the presently accessible resolution.

The deprotonated Asp96 in the M_G state

The FTIR measurements on wild-type samples incubated with GuaHCl reveal another interesting feature of the M_G state. Indeed, changes in the environment of the protonated Asp85, indicated by the positive difference band centred at 1755 cm^{-1}, as well as the deprotonation of Asp96, indicated by the negative difference band at 1742 cm^{-1}, are detectable. This contradicts the assumption that these difference bands are characteristic of the N state (Gerwert *et al.*, 1989; Braiman *et al.*, 1991; Pfefferle *et al.*, 1991). Since the Schiff base is still deprotonated, the proton of Asp96 might have been transferred to a water or a GuaHCl molecule. It suggests that the illuminated sample trapped with GuaHCl is in a state where all changes in the structure and orientation of amino acid residues are as required for the transition to the N state and that only the reprotonation of the Schiff base has not yet taken place; hence the denomination M_G for this state or M_N if samples of the mutant BR-D96N were investigated. GuaHCl thus seems to prevent the direct transfer of the proton to the Schiff base.

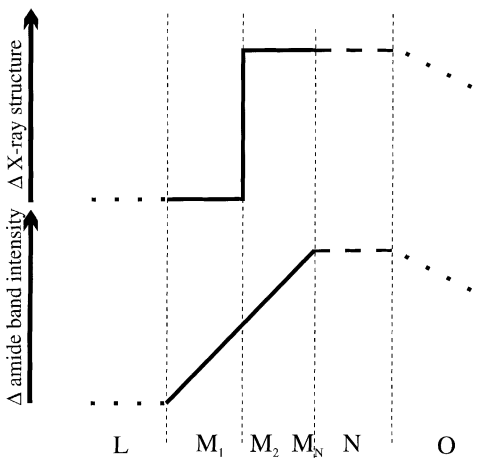

Fig. 6. Schematic diagram of the structural changes during the photocycle of BR as observed in the X-ray diffraction experiment and in the FTIR difference spectra. Solid lines: relative differences determined in the present report; dashed lines: as determined by Pfefferle *et al.* (1991), Sasaki *et al.* (1992), Kamikubo *et al.* (1996) and Vonck (1996); dotted lines: assumed changes.

Structural changes and proton pumping

The importance of the transition from the M_1 to the M_2 state, as indicated by our X-ray experiment as well as in the amide-I region of the FTIR spectra of the dry and hydrated samples, is supported further by proton transport measurements at different hydration levels (Thiedemann *et al.*, 1992). The time course of proton release and re-uptake, as measured with different pH-indicator dyes, was drastically reduced below 75% r.h. Taken together with the diffraction experiments, these results suggest that proton translocation across the membrane is only possible when the large tertiary structure changes can take place. A recent quasi-elastic incoherent neutron study on BR (Fitter *et al.*, 1996) supports the idea that a decrease in hydration results in an appreciable decrease in internal molecular flexibility.

An experiment with mutant Asp85Asn (Kataoka *et al.*, 1994), which revealed structural changes, similar to those seen during the catalytic cycle, upon increasing the pH up to 11 to deprotonate the Schiff base, gave a clear indication that the protonation state of certain groups is of importance in order for the structural changes to take place.

Conclusions

Our results support the following model for the changes (Figure 6) occurring in the M intermediate (M_1, M_2 and M_N/M_G). After isomerization of the retinal upon illumination, the Schiff base is deprotonated and Asp85 protonated concomitantly. This state is called M_1. In this state, the orientation of some amino acid residues changes, preparing the transition to the M_2 state. The onset of the M_2 state is correlated with the change in the tertiary structure of the protein. This large structural change seems to be the result of the proton movement from the Schiff base to Asp85 and the subsequent release of the proton from another group, probably Glu204 (Brown *et al.*, 1995),

to the extracellular side. Thereafter, further changes take place in the orientation of amino acid residues to prepare the release of the proton from Asp96 and the transfer of the proton to the Schiff base. These additional structural changes may be correlated with movements in the inter-helical loops C–D or E–F revealed by spin-labelling (Steinhoff *et al.*, 1994). They occur in the time range of the M decay and could reflect the large additional changes in the amide region in the M_N intermediate. This final M state would display all structural features—large changes in the tertiary structure as well as proper orientation of the amino acids—enabling proton transfer to the Schiff base.

Taking all the results together, a link between the time course of structural changes and that of chemical events can be suggested. The L to M transition causes a charge redistribution by proton transfer from the Schiff base to Asp85 followed by the switch event leading to a change in p*K* and accessibility of the Schiff base. This switch, occurring during the M_1 to M_2 transition, is part of a large conformational change opening the cytoplasmic half-channel for later reprotonation of the Schiff base. Structural changes, not visible by X-ray at the present resolution but monitored by FTIR, continue via M_N until the proton is released from Asp96 (M_G state) and transferred to the Schiff base to form the N intermediate.

Materials and methods

X-ray diffraction experiment

PM were isolated from *Halobacterium salinarium* (S9) or from the mutant *Halobacterium sp.* Asp96Asn (strain 326). PM films for the X-ray measurements were prepared by drying an aliquot of a 30 mg/ml BR solution at 86% r.h. on a mica window at room temperature to obtain an optical density of ~6 at 568 nm. This ensures a reasonable signal-to-noise ratio for the diffraction experiments while still allowing the accumulation of most of the BR molecules in the M state during continuous illumination. Complete accumulation in the M state is easily checked by the colour change from purple to yellow of the sample upon illumination. The humidity was adjusted by incubating a film in a humidity chamber for at least 12 h over an appropriate saturated salt solution (Lide, 1993). Subsequently, the films were enclosed in air-tight sample cells inside an atmos-bag (Aldrich), equilibrated at the required r.h.

X-ray diffraction patterns were recorded at room temperature on beamline X13 of the EMBL in HASYLAB on the storage ring DORIS of the Deutsches Elektronen Synchrotron (DESY) using a linear position sensitive detector with delay line readout (Gabriel and Dauvergne, 1992) and the standard data acquisition system (Boulin *et al.*, 1988). To avoid radiation damage, the sample was continuously translated vertically in the X-ray beam. A small solenoid-driven shutter protected the sample from unnecessary irradiation between data collection periods. Possible radiation damage was checked by collecting the data in successive frames of 30 s each, which were only averaged after validation by statistical comparison with the first frame. The total exposure time did not exceed 600 s. Steady-state illumination was performed with a halogen cold light source equipped with a light guide (Schott, Mainz). A wavelength bandpass from 500 to 800 nm was selected using a combination of an OG515 long pass and a KG1 short pass filter (Schott, Mainz). The X-ray diffraction data were background subtracted and Lorentz corrected by multiplying the experimental intensities by the corresponding values of the scattering vector s ($s = 2*\sin\Theta/\lambda$, where 2Θ is the scattering angle and $\lambda = 1.5$ Å, the wavelength). The diffraction patterns of the films at four different humidities were detected from four different samples. The intensities were scaled with respect to each other by the sum of the integrated reflections in the range from reflection (1,1) to (5,2). Since the samples might have developed different amounts of disorder, this scaling procedure is only roughly true. Part of the scattered intensity might have gone into the incoherent background. Therefore, a comparison of one reflection with the corresponding one in another pattern can only give a qualitative answer. However, a comparison of intensity ratios with and without illumination or of ratios between intensities of different reflections in the same pattern with those at another humidity is quantitatively valid.

Density maps were calculated from the difference amplitudes of the illuminated and the light-adapted ground state samples using phases from electron microscopy (Henderson *et al.*, 1986). The amplitudes of overlapping reflections were determined by splitting the Lorentz-corrected intensities according to the electron microscopy data.

FTIR spectroscopy

For the FTIR measurements, PM films of either wild-type BR or mutant D96N were prepared by applying a 5 µl aliquot of a 10 mg/ml solution to a CaF_2 window and allowing it to stand for a few minutes in air until almost all of the water was evaporated, before transferring it to a humidity chamber where the required r.h. was adjusted for at least 12 h by a saturated salt solution. Before the measurements, the samples were sealed by pressing them tightly in a metal holder together with a greased Teflon spacer ring and a second CaF_2 window.

For incubation with GuaHCl, 20 µl of a 2 M solution (pH 9.6) were deposited on a BR film for at least 1 h in a hydration chamber at 100% r.h. Thereafter, the GuaHCl solution was removed with filter paper. The samples were stored at 100% r.h. before sealing the cell as described above.

FTIR difference spectra were recorded with a Bruker IFS66V spectrometer after baseline stability was ensured. Difference spectra with a resolution of 2 or 4 cm^{-1} were obtained from the average of at least 100 scans in the dark and the average of the immediately following 100 scans under continuous illumination using the same light source as for the X-ray measurements. All measurement were repeated at least three times. Those at low temperatures were performed with an Oxford DN1704 cryostat and repeated after illumination by allowing the samples to warm up above 273 K, before cooling and illuminating again. For comparison, all spectra were scaled to the same Δ-absorbance value at 1201 cm^{-1}.

Acknowledgements

We thank Dr J.Heberle for helpful comments and provision of the FTIR spectrometer. This work was supported by grants from the Deutsche Forschungsgemeinschaft (SFB 312/B4 to N.A.D. and SFB 189/B12, B15 to G.B.), the Bundesministerium für Bildung, Wissenschaft, Forschung und Technologie (03-DE4DAR-1 to N.A.D. and G.B.) and the Fonds der Chemischen Industrie (to N.A.D.).

References

Boulin,C.J., Kempf,R., Gabriel,A. and Koch,M.H.J. (1988) Data acquisition systems for linear and area X-ray detectors using delay line readout. *Nucl. Instrum. Methods*, **A269**, 312–320.

Braiman,M.S., Ahl,P.L. and Rothschild,K.J. (1987) Millisecond Fourier-transform infrared difference spectra of bacteriorhodopsin's M_{412} photoproduct. *Proc. Natl Acad. Sci. USA*, **84**, 5221–5225.

Braiman,M.S., Bousche,O. and Rothschild,K.J. (1991) Protein dynamics in the bacteriorhodopsin photocycle: submillisecond Fourier transform infrared spectra of the L, M and N photointermediates. *Proc. Natl Acad. Sci. USA*, **88**, 2388–2392.

Brown,L.S., Sasaki,J., Kandori,H., Maeda,A., Needleman,R. and Lanyi,J.K. (1995) Glutamic acid 204 is the terminal proton release group at the extracellular surface of bacteriorhodopsin. *J. Biol. Chem.*, **270**, 27122–27126.

Butt,H. J., Fendler,K., Bamberg,E., Tittor,J. and Oesterhelt,D. (1989) Aspartic acids 96 and 85 play a central role in the function of bacteriorhodopsin as a proton pump. *EMBO J.*, **8**, 1657–1663.

Dencher,N.A., Dresselhaus,D., Zaccai,G. and Büldt,G. (1989) Structural changes in bacteriorhodopsin during proton translocation revealed by neutron diffraction. *Proc. Natl Acad. Sci. USA*, **86**, 7876–7879.

Dencher,N.A., Heberle,J., Bark,C., Koch,M.H.J., Rapp,G., Oesterhelt,D., Bartels,K. and Büldt,G. (1991) Proton translocation and conformational changes during the bacteriorhodopsin photocycle: time-resolved studies with membrane-bound optical probes and X-ray diffraction. *Photochem. Photobiol.*, **54**, 881–887.

Ebrey,T.G. (1993) Light energy transduction in bacteriorhodopsin. In Jackson,M.B. (ed.), *Thermodynamics of Membrane Receptors and Channels*. CRC Press, Boca Raton, FL, pp. 353–387.

Fitter,J., Lechner,R.E., Büldt,G. and Dencher,N.A. (1996) Internal

molecular motions of bacteriorhodopsin: hydration-induced flexibility studied by quasielastic incoherent neutron scattering using oriented purple membranes. *Proc. Natl Acad. Sci. USA*, **93**, 7600–7605.

Fodor,S.P., Ames,J.B., Gebhard,R., van den Berg,E.M., Stoeckenius,W., Lugtenburg,J. and Mathies,R. (1988) Chromophore structure in bacteriorhodopsin's N intermediate: implications for the proton-pumping mechanism. *Biochemistry*, **27**, 7079–7101.

Frauenfelder,H. (1995) Complexity in proteins. *Nature Struct. Biol.*, **2**, 821–823.

Gabriel,A. and Dauvergne,F. (1992) The localisation method used at EMBL. *Nucl. Instrum. Methods*, **201**, 203–204.

Gerwert,K., Hess,B., Soppa,J. and Oesterhelt,D. (1989) Role of aspartate-96 in proton translocation by bacteriorhodopsin. *Proc. Natl Acad. Sci. USA*, **86**, 4943–4947.

Han,B.-G., Vonck,J. and Glaeser,R.M. (1994) The bacteriorhodopsin photocycle: direct structural study of two substates of the M-intermediate. *Biophys J.*, **67**, 1179–1186.

Henderson,R., Baldwin,J.M., Downing,K.H., Lepault,J. and Zemlin,F. (1986) Structure of purple membrane from *Halobacterium halobium*: recording, measurement and evaluation of electron micrographs at 3.5 Å resolution. *Ultramicroscopy*, **19**, 147–178.

Heßling,B., Souvignier,G. and Gerwert,K. (1993) A model-independent approach to assigning bacteriorhodopsins's intramolecular reactions to photocycle intermediates. *Biophys. J.*, **65**, 1929–1941.

Kamikubo,H., Kataoka,M., Varo,G., Oka,T., Tokunaga,F., Needleman,R. and Lanyi,J.K. (1996) Structure of the N intermediate of bacteriorhodopsin revealed by X-ray diffraction. *Proc. Natl Acad. Sci. USA*, **93**, 1386–1390.

Kataoka,M., Kamikubo,H., Tokunaga,F., Brown,L.S., Yamazaki,Y., Maeda,A., Sheves,M., Needleman,R. and Lanyi,J.K. (1994) Energy coupling in an ion pump, the reprotonation switch of bacteriorhodopsin. *J. Mol. Biol.*, **243**, 621–638.

Koch,M.H.J., Dencher,N.A., Oesterhelt,D., Ploehn,H.-J., Rapp,G. and Büldt,G. (1991) Time-resolved X-ray diffraction study of structural changes associated with the photocycle of bacteriorhodopsin. *EMBO J.*, **10**, 521–526.

Korenstein,R. and Hess,B. (1977) Hydration effects on the photocycle of bacteriorhodopsin in thin layers of purple membrane. *Nature*, **270**, 184–186.

Korenstein,R., Hess,B. and Kuschmitz,B. (1978) Branching reactions in the photocycle of bacteriorhodopsin. *FEBS Lett.*, **93**, 266–270.

Lanyi,J.K. (1995) Bacteriorhodopsin as a model for proton pumps. *Nature*, **375**, 461–463.

Lide,D.R. (ed.) (1993) *CRC Handbook of Chemistry and Physics*. 74th edn. CRC Press, Boca Raton, FL.

Nakasako,M., Kataoka,M., Amemiya,Y. and Tokunaga,F. (1991) Crystallographic characterization by X-ray diffraction of the M-intermediate from the photocycle of bacteriorhodopsin at room temperature. *FEBS Lett.*, **292**, 73–75.

Oesterhelt,D., Tittor,J. and Bamberg,E. (1992) A unifying concept for ion translocation by retinal proteins. *J. Bioenerg. Biomembr.*, **24**, 181–191.

Ormos,P. (1991) Infrared spectroscopic demonstration of a conformational change in bacteriorhodopsin involved in proton pumping. *Proc. Natl Acad. Sci. USA*, **88**, 473–477.

Ormos,P., Chu,K. and Mourant,J. (1992) Infrared study of the L, M and N intermediates of bacteriorhodopsin using the photoreaction of M. *J. Biochem.*, **31**, 6933–6937.

Perkins,G.A., Liu,E., Burkard,F., Berry,E.A. and Glaeser,R.M. (1992) Characterization of the conformational change in the M_1 and M_2 substates of bacteriorhodopsin by the combined use of visible and infrared spectroscopy. *J. Struct. Biol.*, **109**, 142–151.

Pfefferle,J., Maeda,A., Sasaki,J. and Maeda,A. (1991) Fourier transform infrared study of the N intermediate of bacteriorhodopsin. *Biochemistry*, **30**, 6548–6556.

Sasaki,J., Shichida,Y., Lanyi,J.K. and Maeda,A. (1992) Protein changes associated with reprotonation of the Schiff base in the photocycle of Asp^{96}. *Biol. Chem.*, **267**, 20782–20786.

Schulten,K. and Tavan,P. (1978) A mechanism for the light-driven proton pump of *Halobacterium halobium*. *Nature*, **272**, 85–86.

Steinhoff,H.J., Mollaaghababa,R., Altenbach,C., Hideg,K., Krebs,M., Khorana,H.G. and Hubbell,W.L. (1994) Time-resolved detection of structural changes during the photocycle of spin-labeled bacteriorhodopsin. *Science*, **266**, 105–107.

Subramaniam,S., Gerstein,M., Oesterhelt,D. and Henderson,R. (1993) Electron diffraction analysis of structural changes in the photocycle of bacteriorhodopsin. *EMBO J.*, **12**, 1–8.

Thiedemann,G., Heberle,J. and Dencher,N.A. (1992) Bacteriorhodopsin pump activity at reduced humidity. In Rigaud,J.L.(ed.), *Structures and Functions of Retinal Proteins*. Colloque INSERM/John Libbey Eurotext Ltd, Vol. 221, pp. 217–220.

Varo,G. and Lanyi,J.K. (1990) Pathways of the rise and decay of the M photointermediate(s) of bacteriorhodopsin. *Biochemistry*, **29**, 2241–2250.

Varo,G. and Lanyi,J.K. (1991a) Thermodynamics and energy coupling in the bacteriorhodopsin photocycle. *Biochemistry*, **30**, 5016–5022.

Varo,G. and Lanyi,J.K. (1991b) Kinetic and spectroscopic evidence for an irreversible step between deprotonation and reprotonation of the Schiff base in the bacteriorhodopsin photocycle. *Biochemistry*, **30**, 5008–5015.

Varo,G. and Lanyi,J.K. (1991c) Distortions in the photocycle of bacteriorhodopsin at moderate dehydration. *Biophys. J.*, **59**, 313–322.

Varo,G. and Lanyi,J.K. (1995) Effects of hydrostatic pressure on the kinetics reveal a volume increase during the bacteriorhodopsin photocycle. *Biochemistry*, **34**, 12161–12169.

Varo,G., Zimany,L., Cang,M., Ni,B., Needleman,R. and Lanyi,J.K. (1992) A residue substitution near the β-ionone ring of the retinal affects the M substates of bacteriorhodopsin. *Biophys. J.*, **61**, 820–826.

Vonck,J. (1996) A three-dimensional difference map of the N intermediate in the bacteriorhodopsin photocycle: part of the F helix tilts in the M to N transition. *Biochemistry*, **35**, 5870–5878.

Vonck,J., Han,B.-G., Burkard,F., Perkins,G.A. and Glaeser,R.M. (1994) Two progressive substates of the M-intermediates can be identified in glucose-embedded, wild-type bacteriorhodopsin. *Biophys. J.*, **67**, 1173–1178.

Zimanyi,L., Cao,Y., Chang,M., Ni,B., Needleman,R. and Lanyi,J.K. (1992) The two consecutive M substates in the photocycle of bacteriorhodopsin are affected specifically by the D85N and D96N residue replacements. *Photochem. Photobiol.*, **56**, 1049–1055.

Received on September 16, 1996; revised on December 16, 1996